



# Enhancing Cable-Stayed Bridge Structural Health Assessment Using Phase Space Trajectory and Load Pattern Variability

Mohseni Moghaddam, M. <sup>1a</sup>, Dehghani, E. <sup>2b</sup>, Bitaraf, M. <sup>\*3</sup>

<sup>1</sup> Ph.D. Candidate, Department of Civil Engineering, Faculty of Engineering, University of Qom, Qom, Iran

<sup>2</sup> Associate Professor, Department of Civil Engineering, Faculty of Engineering, University of Qom, Qom, Iran

<sup>3</sup> Assistant Professor, Department of Civil Engineering, Faculty of Engineering, University of Tehran, Tehran, Iran

Received: 07/02/2024

Revised: 06/05/2024

Accepted: 12/06/2024

## Abstract

A novel approach for assessing the structural health of cables in cable-stayed bridges, under varying load patterns, was presented. The method aimed to evaluate cable conditions by utilizing phase space analysis while minimizing traffic disruptions and reducing the necessity for extensive sensor deployment. Through comprehensive numerical investigations on the Manavgat cable-stayed bridge, the efficacy of the proposed method was demonstrated. For this purpose, the time-domain responses of the deck were utilized. The combination of Change in Phase Space Topology

---

\* Corresponding author, E-mail address: [maryam.bitaraf@ut.ac.ir](mailto:maryam.bitaraf@ut.ac.ir)

<sup>a</sup> E-mail address: [M.Mohseni@stu.qom.ac.ir](mailto:M.Mohseni@stu.qom.ac.ir)

<sup>b</sup> E-mail address: [dehghani@qom.ac.ir](mailto:dehghani@qom.ac.ir)

---

(CPST) and Mahalanobis Distance (MD) indexes was applied to detect cable damage by discerning nuanced deviations in phase space trajectories. The results revealed that both the MD and CPST indexes exhibited impressive accuracy in identifying damage severity and location. To emphasize the robustness of the phase space-based damage detection method, a comparative analysis between the CPST and modal parameters was conducted. At the 10% damage level, the accuracy of CPST increased by 84.5% compared to the first mode frequency of the structure in load state 1. It highlighted the high sensitivity of CPST in cable damage detection.

**Keywords:** Cable-stayed bridge, Structural Health Monitoring, Phase Space Method, Damage Detection, Time Domain Responses.

## 1. Introduction

A cable-stayed bridge is a type of bridge where the deck is supported by a system of cables connected to one or more towers. These cables extend directly from the tower to the deck, forming a pattern that resembles a fan or a series of parallel lines. Cable-stayed bridges are widely used for medium to long spans, ranging from 200 meters to well over 1,000 meters. Cable-stayed bridges, noted for their distinctive appearance, structural efficacy, and ability to span significant distances without intermediate piers, are often located in regions where conventional suspension bridge construction is impractical due to geological or environmental constraints. Stay cables, as the main load-bearing components of a bridge, typically account for approximately 25–30% of the total construction cost. Moreover, the cost of replacing cables can be nearly 3-4 times higher than that of new construction (He et al., 2022). As such, ensuring the health of cables throughout the lifespan of the structure and assessing their operational efficiency are paramount concerns, especially for both existing and newly constructed cable-stayed bridges.

---

The practice of Structural Health Monitoring (SHM) for bridges involves continuously collecting and analyzing data about the bridge's condition throughout its operational lifespan. The goal of SHM is to detect and quantify any potential deterioration that may occur during service, while also providing relevant recommendations for maintenance and oversight of the structure. SHM systems typically utilize various sensors, such as accelerometers, strain gauges, and displacement transducers, to capture the structural responses of the bridge to external forces, including traffic, wind, and seismic activity. After data collection, advanced algorithms are employed to analyze the data and identify changes in the structural dynamics of the bridge, including variations in natural frequencies, mode shapes, and damping ratios. This strategic approach enables the early detection of structural impairments, facilitating prompt rectification and maintenance. This technique reduces the risk of catastrophic failures and extends the operational lifespan of the bridge. Furthermore, structural health monitoring helps optimize maintenance schedules and reduce maintenance costs by providing accurate insights into the condition of the bridge (Saidin et al., 2023). In essence, the core of SHM lies in identifying, locating, and quantifying damage through dynamic responses. This comprehensive methodology involves assessing and predicting damage at both local and global levels (Pamwani and Shelke, 2018).

In the field of monitoring performance and ensuring the longevity of engineering structures, the implementation of SHM has provided invaluable insights over extended periods. Over time, numerous numerical and experimental studies have explored the field of cable-stayed bridge health monitoring. The assessment of bridge health and dynamic characteristics in most studies has typically been examined under various environmental conditions, moving loads, artificial vibrations, or stimuli such as earthquakes. Bakhshizadeh et al. (2023) investigated the impact of

---

Multiple Support Excitations (MSE) on the dynamic response of large-span cable-stayed bridges to seismic hazards. Various system identification methods, including mode shape curvature and modal strain energy techniques, were utilized for health monitoring to assess structural performance and identify potential damages (Bakhshizadeh and Sadeghi, 2023).

Numerous researchers have directed their investigations toward ambient vibration (Bedon et al., 2016; Hong et al., 2012). Prawin et al. (2020) introduced a diagnostic scheme for bridges with minimal measurements, considering environmental and operational variations alongside measurement noise. Null subspace analysis was employed in the first stage to confirm the presence of damage using ambient vibration data through online monitoring. It was concluded from the investigations that the proposed approach was capable of detecting and localizing multiple, as well as subtle, damages under varying environmental conditions with very limited noise-contaminated measurements.

Vibration-based methods have played a central role in the field of structural health assessment. A prominent approach is the modal-based damage detection algorithm, which requires the automated identification and continuous tracking of modal parameters for real-time analysis (Li et al., 2014). These methodologies have been validated through comprehensive computational modeling and empirical investigations. A notable study was the work by Saidin et al. (2023), which focused on structural health monitoring using a vibration-based approach for an Ultra-High-Performance Concrete (UHPC) bridge. In this study, researchers extracted mode shapes, natural frequencies, and damping ratios to understand the modal characteristics of the bridge. These parameters were then used to assess the bridge's performance and monitor its health over time. The main objective of this study was to highlight the effectiveness of SHM in detecting structural impairments and predicting the behavior of engineering structures.

---

Also, Vibration-based methodologies are extensively utilized for estimating cable tension and evaluating the comprehensive health of cable structures. Fatigue and corrosion have presented recurring challenges that can affect cables, leading to decreased stiffness and compromised force transmission. Therefore, monitoring tension, as the primary indicator of cable health, is of paramount importance. This consideration arises from the relationship between cable tension, its strength, and stiffness. Cable tension can be determined using various methodologies, including direct force sensor measurements, non-contact measurements, or assessments of parameters like stress, strain, or natural frequency (Cheng et al., 2024; Fathali et al., 2020; Rinaldi et al., 2023; Yu, 2020). An illustrative example is the study conducted by Zarbaf et al. (2018), who utilized this technique to evaluate the cables of the Ironton-Russell Bridge. Their findings were subsequently compared with those obtained from lift-off tests. These approaches have utilized the natural frequencies, mechanical properties, and geometric features of cables to estimate tension. Jana et al. (2022) introduced a framework that utilized video-based measurements as multiple sensors to minimize estimation errors in real-time cable tension determination. Non-contact video-based sensing offered superior spatial resolution and lower costs compared to conventional sensors. The algorithm was implemented on the Fred-Hartman cable-stayed bridge in Texas, demonstrating accurate tension estimation from video-based measurements. This showcased the significant potential of the framework in structural health monitoring.

Damage detection methods under moving load can be categorized into two methods: frequency domain method and time domain method (He et al., 2017; Wu et al., 2017, 2019). While frequency measurement provides high precision, it tends to offer a global perspective. It has posed challenges for local damage detection. Conversely, mode shape and its derivatives, such as modal curvature and modal flexibility, have theoretically shown sensitivity to damage. However, they are often

---

affected by measurement noise, compromising their reliability in practical civil structural health monitoring scenarios when using displacement or acceleration data (Hong et al., 2012; Wu et al., 2017). In some investigations, Time Domain Responses (TDR) have proven to be effective tools for identifying localized damage. TDR-based methods directly identify damage from the output, bypassing the need for conversion into structural modal information. Zhang et al. (2020) introduced a rapid output-only technique for detecting damage in highway bridges under moving vehicles, relying on the fractal dimension of long-gauge FBG strain responses. The feasibility of both single and multiple damage scenarios was demonstrated through numerical simulations and an indoor bridge-vehicle model experiment. Additionally, the method's resistance to noise was assessed by adding a signal-noise ratio (SNR) of 30 dB in the numerical simulation, and the impact of varying sensor quantities was investigated. In another study, Kordi and Mahmoudi (2022) presented a new method for detecting damage in truss bridges under moving loads. Damage was identified by comparing the displacement response curve shapes of the intact and damaged models with the axial force influence line curve shape. The results showed that the proposed method can accurately identify the damaged members.

Cable-stayed bridges are renowned for their flexibility. In this structural configuration, the girder operates like a beam resting on a flexible foundation, while the cables provide flexible support from their anchoring points. The primary load paths across the bridge deck provide valuable insights into the condition of secondary structural elements, such as the stay cables. Nazarian et al. (2016) introduced a straightforward approach to recognizing damage in the cables of cable-stayed bridges. This method involved monitoring variations in support reactions by analyzing shear forces acting upon deck components near the support locations. The researchers also proposed a technique to identify cables that have experienced partial or complete loss of

---

tensile force, achieved by measuring strains along the bridge deck. It is important to acknowledge that this technique may face challenges in accurately modeling geometric constraints and boundary conditions, potentially resulting in inaccuracies.

Displacements of the main beam and towers are key indicators of bridge performance, commonly tracked using Global Positioning System (GPS) sensors. For example, in long-span cable-stayed bridges, these displacements are often measured statically during load testing before the bridge is opened to traffic. Although acceleration measurements can also provide displacement data, their precision is lower (Zhang et al., 2023). Additionally, various factors such as temperature fluctuations, wind forces, and vehicular traffic impact the displacement of long-span bridges. Lei et al. (2023) proposed an approach involving the use of a one-dimensional residual convolutional autoencoder model to estimate displacement responses of a cable-stayed bridge under various loading conditions. To implement this approach, the researchers collected monitoring data from a cable-stayed bridge, including comprehensive measurements of varied loads and corresponding displacement responses. Subsequently, temperature, wind, and vehicle load characteristics were used as input variables, while the displacement responses at the mid-span of the main girder and the tops of the two pylons were used as output variables. The model underwent training and validation procedures using the collected monitoring data. It achieved an accuracy exceeding 95% in predicting a range of displacement responses associated with multiple critical loads, all used simultaneously as inputs.

Within the field of civil engineering, phase space analysis has emerged as a valuable tool for damage detection. This methodology initially relies on strain history data, transforming time series data into a spatial domain, where even slight changes in parameters can propagate throughout the

---

entire system. The Change in Phase Space Topology (CPST) index has been introduced as an immensely effective method, capable of increasing in value proportionally to the severity of damage, regardless of its location (Nie et al., 2012, 2013). Zhang et al. (2017) introduced a model-free method for detecting damage in bridge structures under moving loads, relying on changes in phase trajectory across multiple vibration measurements. The sensitivity and reliability of this approach were examined through numerical analysis of a simply supported beam structure. Experimental validation revealed that shear connection failures in a composite bridge structure model subjected to moving loads were effectively identified by the method.

In multidimensional statistical analysis, the Mahalanobis Distance (MD) is another index that refers to a measure of distance on the scale of standard deviation between an observation and a reference sample. Like CPST, it has been introduced as a damage index in studies related to health monitoring (De Maesschalck et al., 2000; Pamwani and Shelke, 2018). The significant sensitivity of phase space analysis to damage has made it widely used in various studies on structural damage detection (Li et al., 2021; Paul et al., 2017; Peng et al., 2022; Tuttipongsawat et al., 2019).

According to the studies, modal parameters such as natural frequency have shown limited sensitivity to local damages in bridges. Additionally, vibration-based methods for detecting damage have often disrupted traffic flow or required complete bridge closures if necessary. In examining the structure's behavior in the frequency domain, time is also dedicated to converting responses from the time domain to the frequency domain, resulting in a large volume of data. In the literature review on moving loads, the assessment of structural health has typically been conducted using a single type of load pattern. In this article, a novel approach was introduced for tracking cable health in cable-stayed bridges subjected to various load patterns. The approach included a comprehensive examination of phase space reconstruction and damage-sensitive

---

indexes. This method observed how the structure behaves over time with minimal traffic disruptions or bridge closures, achieved by applying a specific load. The need for multiple and costly sensors was removed throughout the bridge deck using displacement sensors or non-contact methods. In this study, a rapid method was provided for early damage detection in cable-stayed bridges, by using only one type of response. The research conducted in the realm of damage detection using phase portraits has often focused on structures such as frames, buildings, and highway bridges. In this research, the efficacy of phase space analysis was assessed on a cable-stayed bridge using both the change in phase space topology and the Mahalanobis distance indexes. A cable-stayed bridge located in Turkey, featuring a steel pylon, a composite deck, and 28 steel cables, was investigated. Numerous damage scenarios, encompassing distinct load patterns and speeds, were evaluated. The proposed method involved reconstructing the deck's displacement at the cable connection points in the phase space and subsequently examining the resulting damage indexes.

## **2. Methods**

### **2.1. Phase Space Reconstruction**

Phase space analysis is a novel method for structural damage detection. The method demonstrates exceptional sensitivity to damage because it magnifies changes in time-domain responses by converting them into a spatial domain. In phase space, each variable represents a distinct dimension in a multi-dimensional space, indicating that any change in one parameter will propagate throughout the entire system. Dynamic systems can be defined by their measured time-series responses in phase space. The phase space can be reconstructed using multiple variables or

---

the time series of a single measured variable, incorporating parameters such as time lag ( $T$ ) and embedding dimension ( $d$ ) (Takens, 1981).

Given a time series measurement denoted as  $x(i)$  with  $N$  data points (where  $i = 1, \dots, N$ ), the reconstruction of the phase space can be formulated as follows (Tuttipongswat et al., 2019):

$$X(n) = [x(n), x(n + T), \dots, x(n + (d - 1)T)] \quad (1)$$

Each dimension can be expressed as:

$$\begin{aligned} x(n) &= [x(1), x(2), \dots, x(N - (d - 1)T)] \\ x(n + T) &= [x(1 + T), x(2 + T), \dots, x(N - (d - 2)T)] \\ &\vdots \\ x(n + (d - 1)T) &= [x(1 + (d - 1)T), x(2 + (d - 1)T), \dots, x(N)] \end{aligned} \quad (2)$$

The set of all dimensions plotted is called phase space topology. The geometry of the phase trajectory is closely related to the behavior of the structure. Any damage to the structure leads to changes in responses, which are accurately depicted in the topology of the phase space. By assessing the dissimilarity of the topology when damage occurs, it is possible to detect the presence of damage. Selecting an appropriate time lag is crucial during the reconstruction process. The time lag can be determined using methods such as the Autocorrelation Function and the Average Mutual Information Function (AMIF). Typically, the lag for reconstruction is chosen as the time corresponding to the first zero crossing of the Autocorrelation Function or the first minimum of the AMIF (Abarbanel, 2012; Jiang et al., 2010). Similarly, the optimal choice of the embedding dimension ( $d$ ) is essential in the reconstruction process. Prominent techniques used to determine the appropriate embedding dimension include Singular System Analysis (SSA) and False Nearest Neighbor (FNN) methods (Broomhead and King, 1986; Nichols, 2003; Rhodes and Morari, 1997). In this study, the Average Mutual Information Function and False Nearest Neighbor methods were employed to determine the time lag and embedding dimension, respectively.

---

## 2.2. Damage Sensitive Feature

In this study, the relationship between the geometry of the phase space trajectory and the dynamic response of the structure was discussed. As damage gradually occurs, discernible changes are triggered within the dynamic response, which are distinctly reflected in the topology of the phase space. Two damage indexes were used for damage detection in cable-stayed bridges: the Change in Phase Space Topology (CPST) and the Mahalanobis Distance (MD) between phase space trajectories. These indexes have been proposed as valuable tools for evaluating the health of the structure using phase space analysis (Nichols, 2003).

### 2.2.1. Change in Phase Space Topology (CPST)

The CPST index concept aims to measure the difference between the predicted damage case and the actual damage case. assume  $\mathbf{X}(\mathbf{n})$  and  $\mathbf{Y}(\mathbf{n})$  are phase space reconstructions of a healthy case and a damaged case, respectively. The calculation concept is illustrated in Figure 1 (Tuttipongswat et al., 2019). To begin, a fiducial point  $Y(r)$  at time index  $r$  from the damage case is selected, and mapped on the healthy case. By minimizing the Euclidean norm, the nearest  $p$  neighbors of this fiducial point are chosen on the healthy case (Nie et al., 2013; Pamwani and Shelke, 2018; Tuttipongswat et al., 2019):

$$NN(n_j): \min \|X(n_j) - Y(r)\|, \quad j = 1, \dots, p \quad (3)$$

Here,  $P$  denotes the total number of neighborhood points, and the operator  $\|\bullet\|$  calculates the Euclidean norm. The set of nearest neighbor points to the fiducial point  $Y(r)$  is denoted as  $NN$ . These selected neighborhood points are used to quantify the dissimilarity between the healthy and

damaged cases. The predicted damage case at the 's' time step can be computed using Eq. (4) (Nie et al., 2013; Pamwani and Shelke, 2018; Tuttipongsawat et al., 2019).

$$\hat{Y}(r+s) = \frac{1}{p} \sum_{j=1}^p X(n_j+s), \quad j = 1, \dots, p \quad (4)$$

Hence, the difference between the damage case  $Y$  and the predicted damage case  $\hat{Y}$  of the fiducial point at time index  $r$  is determined as shown in Eq. (5) (Nie et al., 2013; Pamwani and Shelke, 2018; Tuttipongsawat et al., 2019).

$$\text{CPST}(i) = \frac{1}{p} \left\| \hat{Y}(r+s) - Y(r+s) \right\|, \quad i = 1, \dots, nt \quad (5)$$

The calculation process will be repeated to obtain an average value of the CPST difference. The number of repetitions or fiducial points is denoted as  $nt$ . It is recommended to choose at least 5% of the total number of points in the reconstructed trajectory as the number of fiducial points to achieve a reasonable estimate of CPST (Nichols, 2003). In some references, the number of fiducial points is calculated using Eq. (6) (Nie et al., 2013).

$$nt = N - (d-1)T \quad (6)$$

Where  $N$ ,  $d$ , and  $T$  represent the total number of data points, embedding dimension, and time lag of reconstruction, respectively.

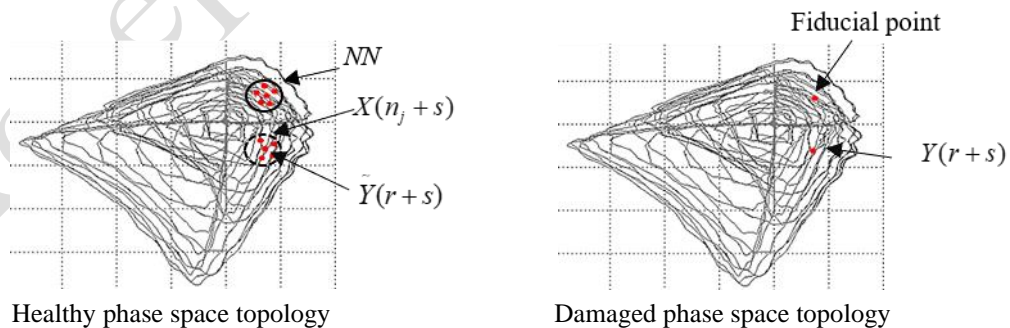


**Fig. 1.** Diagram of CPST calculation process

### 2.2.2. Mahalanobis Distance (MD)

---

The Mahalanobis Distance (MD) is commonly utilized to measure the distance of an individual point from a cluster of points and evaluate its deviation from the overall population. The observations of the coordinate vectors for each point from the healthy and damaged cases are represented in matrix form as  $[\mathbf{X}]$  and  $[\mathbf{Y}]$ , respectively. The matrices are of dimensions  $(m \times d)$ , where 'm' is the number of points sampled on the embedded phase portrait, equal to the number of rows. The number of columns 'd' represents the number of embedding dimensions. The healthy and damaged phase portraits are represented by two random vectors,  $\{\mathbf{X}\}$  and  $\{\mathbf{Y}\}$ , respectively. The centroid of these portraits is obtained by calculating the mean of these random vectors, denoted as  $\{\mu\}_x$  and  $\{\mu\}_y$ , respectively. Their covariance matrices can also be estimated as  $[C_{xx}]$  and  $[C_{yy}]$ , respectively. To compute the MD, a single weighted covariance matrix is derived by assigning relative weights to each of these covariance matrices. This is expressed as (George et al., 2018) :

$$[C_{ww}] = W_1[C_{xx}] + W_2[C_{yy}] \quad (7)$$

The weight factors are determined based on the ratio of the number of points sampled in each phase portrait to the total number of points sampled in both. In this paper, equal weights were assigned to each covariance matrix,  $w_1 = w_2 = 0.5$ . The Mahalanobis Distance (MD) between the phase portraits is calculated using the following formula (George et al., 2018):

$$MD = \sqrt{(\{\mu\}_x - \{\mu\}_y)^T [C_{ww}] (\{\mu\}_x - \{\mu\}_y)} \quad (8)$$

This modified version of the MD was used as a damage index in this study. More detailed information on MD calculation can be found in the reference (George et al., 2018).

### 3. Case Study

The Manavgat cable-stayed bridge, shown in Figure 2, was selected for numerical analysis. This bridge is Turkey's first cable-stayed bridge, designed to accommodate two lanes of road traffic.

The bridge is 202 meters long, with each span measuring 101 meters. It features a 13.7-meter-wide deck connected to a steel tower by 28 cables. The tower stands approximately 42 meters high and has a hollow hexagonal cross-section, mounted on a concrete foundation. The deck is constructed with a composite cross-section, comprising 25 cm of concrete, 10 cm of asphalt, and two continuous steel girders that are laterally restrained. I-shaped steel profiles are embedded continuously along the length of the deck. The deck is supported by 28 steel cables, which are interconnected with the tower. The nearest cable to the pylon is 19.6 meters away, with a distance of 12 meters between each subsequent cable. The last cables are situated 9.4 meters from the supports. The arrangement of the cables, as well as the cross sections of the deck and the pylon, are shown in Figure 3 (Pan et al., 2018).



**Fig. 2.** Manavgat cable-stayed bridge (Elkady et al., 2023)

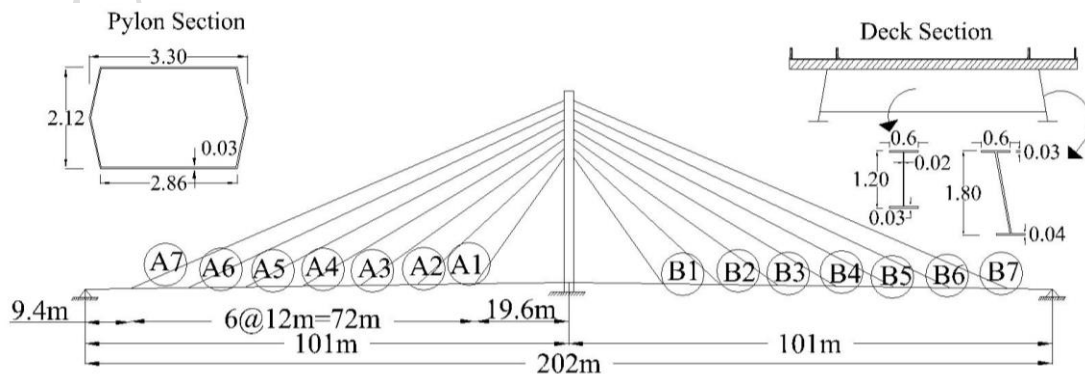


**Fig. 3.** Manavgat cable-stayed bridge arrangement and the cross-section of the bridge members

### 3.1. Finite Element Modeling

For the assessment of the structural behavior of the Manavgat cable-stayed bridge, a three-dimensional finite element model was created utilizing SAP2000 software. The deck and pylon were modeled using frame elements and the pylon was fixed to the foundation. Truss elements were used for the cables. The details of the stay cables, labeled A1-A7 and including 14, 16, 19, 19, 22, 19, and 24 strands respectively, are provided in Table 1 (Pan et al., 2018). Each strand has an elastic modulus of 197 GPa, a cross-sectional area of  $150_{mm^2}$ , and an ultimate strength of 1,860 MPa. Moreover, the elastic moduli for the concrete and steel materials were specified as 34 GPa and 200 GPa, respectively.

**Table 1.** Numbering and details of stay cables

Cable number	Cable name	Number of strands	Total area of cable ( $_{mm^2}$ )
1	A7	24	4355
2	A6	19	3448
3	A5	22	3992
4	A4	19	3448
5	A3	19	3448
6	A2	16	2903
7	A1	15	2722
8	B1	15	2722
9	B2	16	2903
10	B3	19	3448
11	B4	19	3448
12	B5	22	3992
13	B6	19	3448
14	B7	24	4355
15	A7	24	4355
16	A6	19	3448
17	A5	22	3992
18	A4	19	3448
19	A3	19	3448
20	A2	16	2903
21	A1	15	2722

22	B1	15	2722
23	B2	16	2903
24	B3	19	3448
25	B4	19	3448
26	B5	22	3992
27	B6	19	3448
28	B7	24	4355

To simulate the interaction between the bridge and vehicle, examples of a five-axle and a two-axle truck, similar to the AASHTO standard load, were employed in the finite element bridge model, as illustrated in Figure 4 (AASHTO, 2008). This five-axle truck is also specified in the Australian Bridge Design Code as T44 (Australasian Railway Association, 1992). The analysis of the bridge under moving load was conducted using simulated time history analysis in SAP2000 software. The moving load was applied to the deck through the distribution of multiple point loads at uniform intervals. Breaking down the moving load into multiple point loads and their corresponding time history function is illustrated in Figure 5.

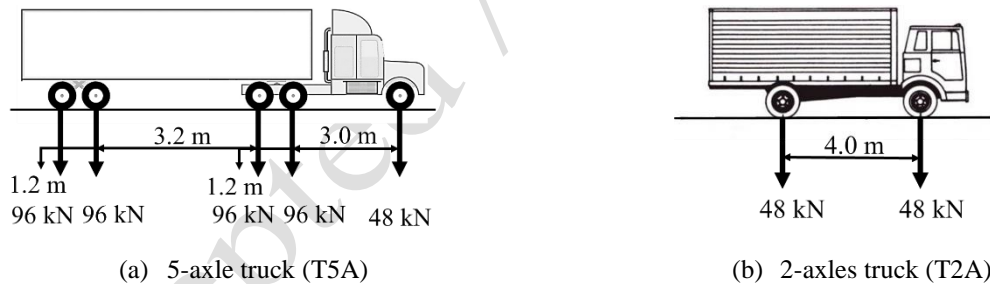


**Fig. 4.** Truck loadings for 3D model analysis

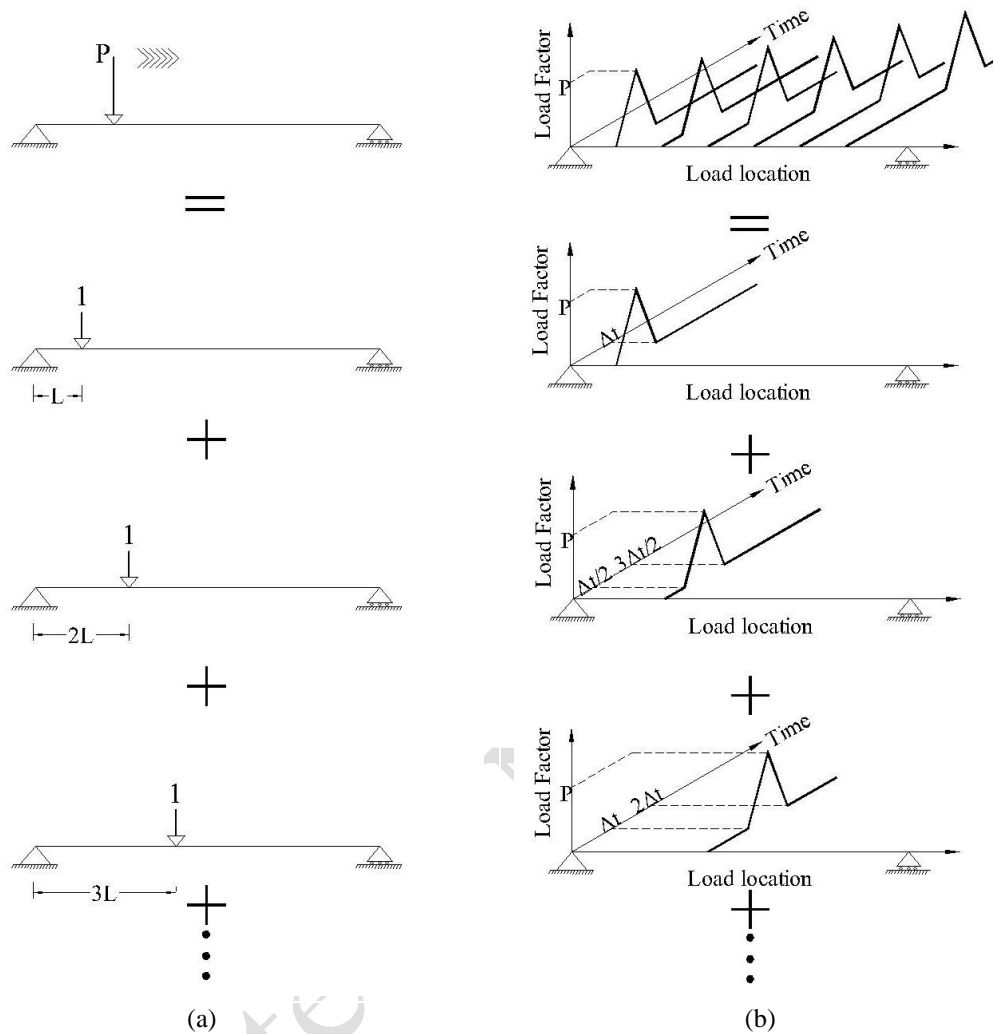


**Fig. 5.** Breaking down: (a) the moving load into point loads at uniform intervals and (b) the time history functions

Point loads, following the load pattern depicted in Figure 5, were applied and removed from the deck. Loads were successively passed over the bridge, with  $\Delta t$  determined by the formula below:

$$\Delta t = \frac{L}{V} \quad (9)$$

$L$  denotes the distance between point loads, while  $V$  indicates the speed of the moving load.

## 4. Results and Discussion

As mentioned, the deck girder in cable-stayed bridges functions like a beam supported by elastic foundations, owing to the presence of cables. The changes in the deck's response provide crucial insights into the condition of the stay cables. In this paper, a time history analysis was performed, involving a round-trip truck at an average speed of 10-15 Km/h. Dynamic effects were ignored in the analysis. The evaluation of the vertical displacement of the deck at the points of cable attachment was conducted to assess the health of the cable-stayed bridge. The displacement of each point was reconstructed using parameters of time lag and embedding dimension, extracted from the displacement vector in the phase space. To identify damaged cables through disparities in phase space trajectories between healthy and damaged cases, two distinct damage indexes were utilized: the Change in Phase Space Topology (CPST) and the Mahalanobis Distance (MD). This paper aimed to detect damage within the cables of cable-stayed bridges using two distinct loading types. A comprehensive overview of the methodology is outlined in the workflow depicted in Figure 6.

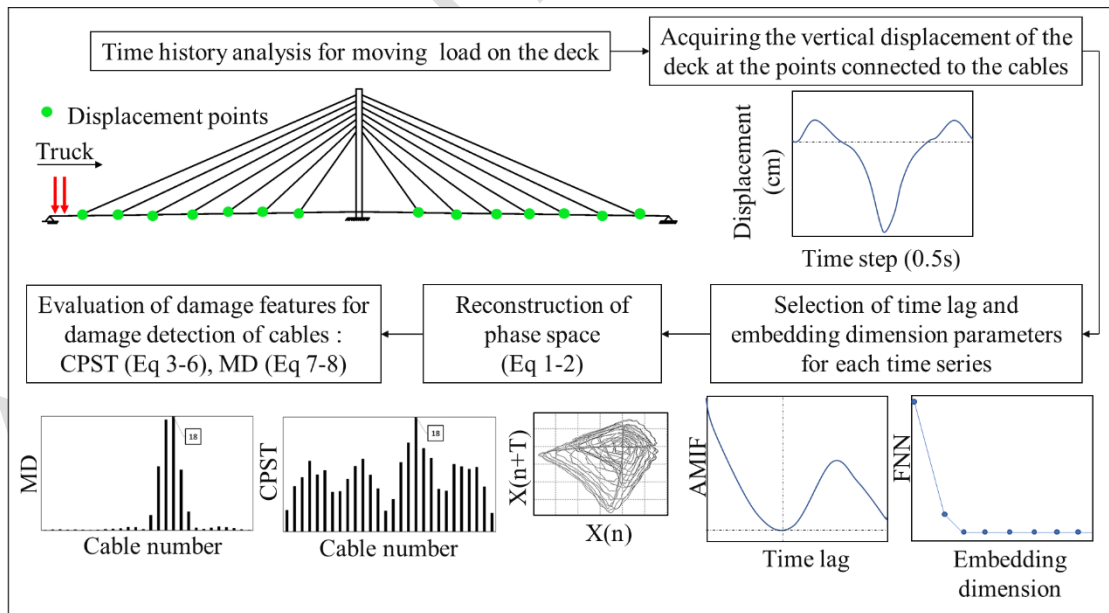


**Fig. 6.** Workflow of the proposed damage detection method

The process of damage detection typically involves the comparison of two cases: one healthy and the other damaged. In this study, the first investigation of cable damage detection was focused on five distinct cable damage scenarios under ideal conditions. The term 'ideal conditions' indicates that the passing load was consistent in both the healthy and damaged cases. The speed of the passing load was variable in the three damage scenarios. The extent of damage varied from a reduction of 10% to 45% in the cross-sectional area of the cables. After reconstructing the phase space of deck displacements at the cable connection points, the two damage indexes, MD and CPST, were computed and presented in Table 2. The discussion of these indexes can be found in the 'Damage Sensitive Feature' section.

Except cable 1, both MD and CPST indexes (or at least one of them) accurately identified the damaged cables, namely cables 6, 11, 18, and 25. Cable 1, which acted as a backstay cable supporting all the bridge cables, remained undetected even with a significant damage intensity of 45%. Damage to this cable has affected all other cables. It is important to note that the index values are normalized to the highest value for ease of evaluation.

Cables 1, 2, 13, 14, 15, 16, 27, and 28 were categorized as backstay cables. The damage detection index curve for cable 18 is illustrated in Figure 7. In this particular scenario, the speed of the passing load in the healthy case was 10 Km/h, while in the damaged case, it was 15 Km/h. The results were examined under a 5-axle truck (T5A).

**Table 2.** Damage scenarios under ideal conditions

Cable number	Passing load (intact/damaged)	Passing speed (intact/damaged) Km/h	Damage percentage (%)	Mahalanobis distance (MD)	Change in phase space topology (CPST)
1	T5A/T5A	10/10	45	26	26
6	T5A/T5A	10/10	40	5	6
11	T2A/T2A	15/15	10	11	11
18	T5A/T5A	10/15	30	18	18
25	T2A/T2A	15/10	30	25	17

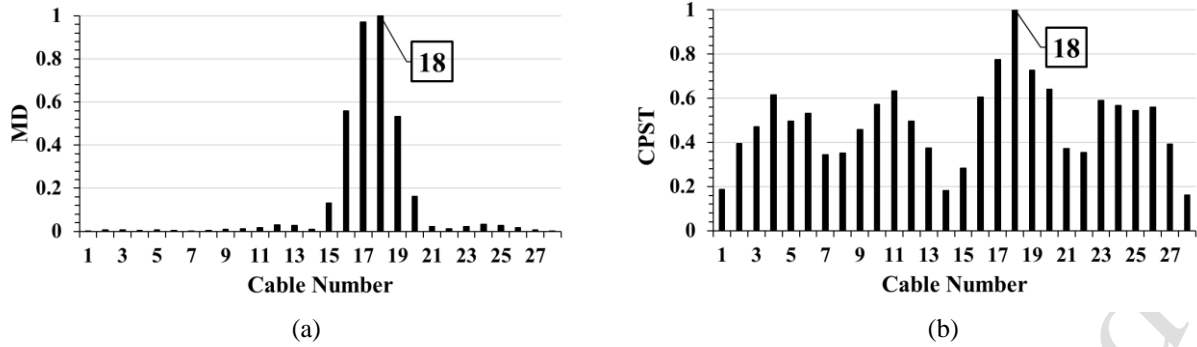


**Fig. 7.** Damage detection curves for cable 18: (a) MD; (b) CPST

The second part of the considered damage scenarios involved the passage of trucks with varying load patterns and speeds in both healthy and damaged cases. The severity of damage in these scenarios varied from 20% to 40% of the cable cross-sectional area. These scenarios were analyzed across five distinct states, as shown in Table 3.

In the first state, the passing load in the healthy case was the 2-axle truck (T2A), while in the damaged case, the displacements were acquired from the passage of the 5-axle truck (T5A). The passing speed for both trucks in this state remained consistent at 10 Km/h. In the second state, data were examined for the passage of the T5A truck at 15 Km/h in the healthy case and the passage of the T2A truck at 10 Km/h in the damaged case. The third state was the opposite of the second one, where the trucks passing in the healthy and damaged cases changed places, but the passing speeds remained the same as in the second state. In the fourth state, the T5A truck was used at 10 km/h in the healthy case, whereas the T2A truck was utilized at 15 km/h in the damaged case. In the fifth state, the trucks were opposite to those in the fourth state, but the passing speeds remained the same as in the fourth state.

All cables, except for the backstay cables (totaling 20 cables), were analyzed and examined under these five states, each with three different levels of damage intensity: 20%, 30%, and 40%.

The aim of examining the cables in these scenarios was to assess how well the damage detection method performs when exposed to various load patterns. The results of the damage detection indexes for cable cross-section damage levels of 20%, 30%, and 40% under the five different states are presented in Tables 4, 5, and 6, respectively.

**Table 3.** Five states of load passing scenarios

	Intact		Damaged	
	Passing load	Passing speed Km/h	Passing load	Passing speed Km/h
State 1	T2A	10	T5A	10
State 2	T5A	15	T2A	10
State 3	T2A	15	T5A	10
State 4	T5A	10	T2A	15
State 5	T2A	10	T5A	15

As depicted in Figure 8, To maintain uniformity in the number of data points for phase space analysis resulting from the passage of different trucks at various speeds, the arrival and departure times of the resultant load were considered. Additionally, since the load values of the axles in the trucks were different, all initial data were normalized to the maximum displacement at the middle point of the bridge span.

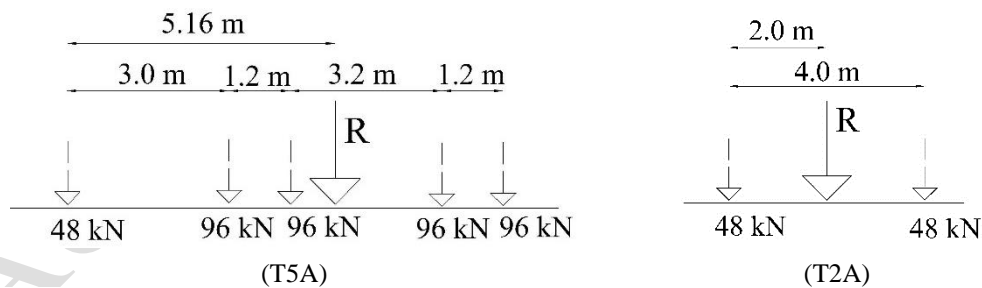


**Fig. 8.** Resultant load for T5A and T2A trucks

**Table 4.** Results of damage detection for damage level of 20%, excluding backstay cables

Cable number	State 1		State 2		State 3		State 4		State 5	
	MD	CPST								
3	3	3	3	25	17	16	3	12	3	17
4	3	4	4	26	17	17	3	12	4	17

<b>5</b>	4	18	<b>5</b>	25	17	18	12	12	4	<b>5</b>
<b>6</b>	5	<b>6</b>	26	12	17	12	12	12	5	5
<b>7</b>	12	3	26	11	26	17	12	12	12	3
<b>8</b>	25	3	3	11	12	12	17	17	9	3
<b>9</b>	25	24	3	3	12	12	17	12	25	26
<b>10</b>	25	11	<b>10</b>	3	12	12	17	12	11	11
<b>11</b>	26	26	<b>11</b>	3	12	12	26	12	26	26
<b>12</b>	26	25	<b>12</b>	26	<b>12</b>	<b>12</b>	26	17	<b>12</b>	<b>12</b>
<b>17</b>	3	16	<b>17</b>	26	<b>17</b>	16	3	<b>17</b>	<b>17</b>	<b>17</b>
<b>18</b>	3	<b>18</b>	<b>18</b>	25	17	16	3	12	3	17
<b>19</b>	3	18	<b>19</b>	25	17	18	12	12	18	4
<b>20</b>	4	4	26	12	17	17	12	12	5	5
<b>21</b>	12	26	26	12	26	16	12	12	12	26
<b>22</b>	25	<b>22</b>	3	25	12	12	17	12	24	26
<b>23</b>	25	24	3	3	12	17	17	13	24	24
<b>24</b>	25	<b>24</b>	<b>24</b>	3	12	17	17	12	25	25
<b>25</b>	26	26	<b>25</b>	3	12	13	26	13	<b>25</b>	11
<b>26</b>	<b>26</b>	<b>26</b>	<b>26</b>	17	12	12	<b>26</b>	11	<b>26</b>	12

**Table 5.** Results of damage detection for damage level of 30%, excluding backstay cables

Cable number	State 1		State 2		State 3		State 4		State 5	
	MD	CPST								
<b>3</b>	<b>3</b>	2	<b>3</b>	<b>3</b>	<b>3</b>	4	13	13	<b>3</b>	4
<b>4</b>	<b>4</b>	<b>4</b>	<b>4</b>	<b>4</b>	17	12	<b>4</b>	12	<b>4</b>	18
<b>5</b>	4	4	<b>5</b>	26	17	17	4	12	4	4
<b>6</b>	5	<b>6</b>	26	25	17	18	12	12	5	5
<b>7</b>	12	26	26	3	26	17	12	17	26	3
<b>8</b>	9	<b>8</b>	3	25	3	12	17	12	9	<b>8</b>
<b>9</b>	24	24	10	3	12	17	17	12	10	10
<b>10</b>	25	<b>10</b>	<b>10</b>	<b>10</b>	12	11	25	12	11	<b>10</b>
<b>11</b>	26	10	<b>11</b>	18	12	17	26	12	<b>11</b>	12
<b>12</b>	26	26	<b>12</b>	<b>12</b>	<b>12</b>	<b>12</b>	26	<b>12</b>	<b>12</b>	<b>12</b>
<b>17</b>	3	3	<b>17</b>	<b>17</b>	<b>17</b>	16	3	12	<b>17</b>	<b>17</b>
<b>18</b>	<b>18</b>	<b>18</b>	<b>18</b>	19	17	<b>18</b>	<b>18</b>	19	<b>18</b>	<b>18</b>
<b>19</b>	4	18	18	18	17	13	4	12	18	<b>19</b>
<b>20</b>	5	<b>20</b>	26	26	17	17	12	13	19	<b>20</b>
<b>21</b>	12	12	26	26	26	12	12	12	12	17
<b>22</b>	23	23	3	12	12	17	17	12	23	<b>22</b>
<b>23</b>	24	24	3	3	12	12	17	12	24	24
<b>24</b>	25	<b>24</b>	<b>24</b>	3	12	12	25	12	25	<b>24</b>
<b>25</b>	<b>25</b>	26	<b>25</b>	<b>25</b>	12	13	<b>25</b>	17	<b>25</b>	26
<b>26</b>	<b>26</b>	<b>26</b>	<b>26</b>	<b>26</b>	12	17	<b>26</b>	12	<b>26</b>	<b>26</b>

**Table 6.** Results of damage detection for damage level of 40%, excluding backstay cables

Cable number	State 1		State 2		State 3		State 4		State 5	
	MD	CPST	MD	CPST	MD	CPST	MD	CPST	MD	CPST
<b>3</b>	<b>3</b>	<b>3</b>	<b>3</b>	<b>3</b>	17	16	<b>3</b>	18	<b>3</b>	2
<b>4</b>	<b>4</b>	3	<b>4</b>	<b>4</b>	17	16	<b>4</b>	12	<b>4</b>	<b>4</b>
<b>5</b>	4	4	4	<b>5</b>	4	<b>5</b>	4	<b>5</b>	4	<b>5</b>
<b>6</b>	5	<b>6</b>	26	12	17	12	12	12	5	<b>6</b>

---

7	12	3	26	26	26	17	12	17	26	26
8	10	10	10	15	10	18	17	12	10	9
9	24	9	10	3	12	12	17	12	10	24
10	25	10	10	10	12	11	25	12	11	10
11	11	25	11	11	12	12	25	17	11	12
12	12	12	12	12	12	12	26	17	12	26
17	17	2	17	17	17	17	3	12	17	17
18	18	17	18	18	17	12	3	18	18	17
19	4	19	19	19	17	17	4	12	18	19
20	19	20	26	25	17	18	12	16	19	20
21	12	26	26	25	26	18	12	12	26	3
22	23	22	3	27	3	12	17	17	23	22
23	24	24	23	18	12	17	17	13	24	23
24	25	24	24	10	12	11	25	12	25	25
25	25	26	25	25	12	12	25	12	25	26
26	26	26	26	26	12	13	26	13	26	13

---

The damage indexes, especially MD, accurately detected damaged cables at different levels of damage in specific cases, such as cables 3, 12, 17, and 26. Furthermore, in several cases involving cables 5, 10, 18, 19, 23, and 24, the MD index frequently indicated the damaged cable with a difference of one cable before or after it. However, in many cases involving cables near the pylon (cables 7, 8, 21, and 22), the indexes failed to detect the damage using this method, resulting in inconclusive outcomes. Notably, more favorable results were obtained for damage levels of 30% and higher.

The MD and CPST curves for the 40% damage level of cables 5 and 21 are presented in Figures 9-12. The choice of cable 5 was an example of cables for which the indexes often detected a cable before or after the damaged cable in most states. Cable 21 was selected as one of the four nearest cables to the pylon that could not be identified through this method. Although in cases like cables 8 and 22 in the fifth state at damage levels of 30% and 40%, CPST correctly detected the damaged cables, it's worth noting that the accuracy of this method was limited. In addition, the values of the indexes in states two and five for all scenarios showed that the changes in other cables, except the damaged cable, were relatively less compared to the other states. In essence, when the T5A truck

passed at a higher speed than the T2A, the changes observed in the other cables were less pronounced.

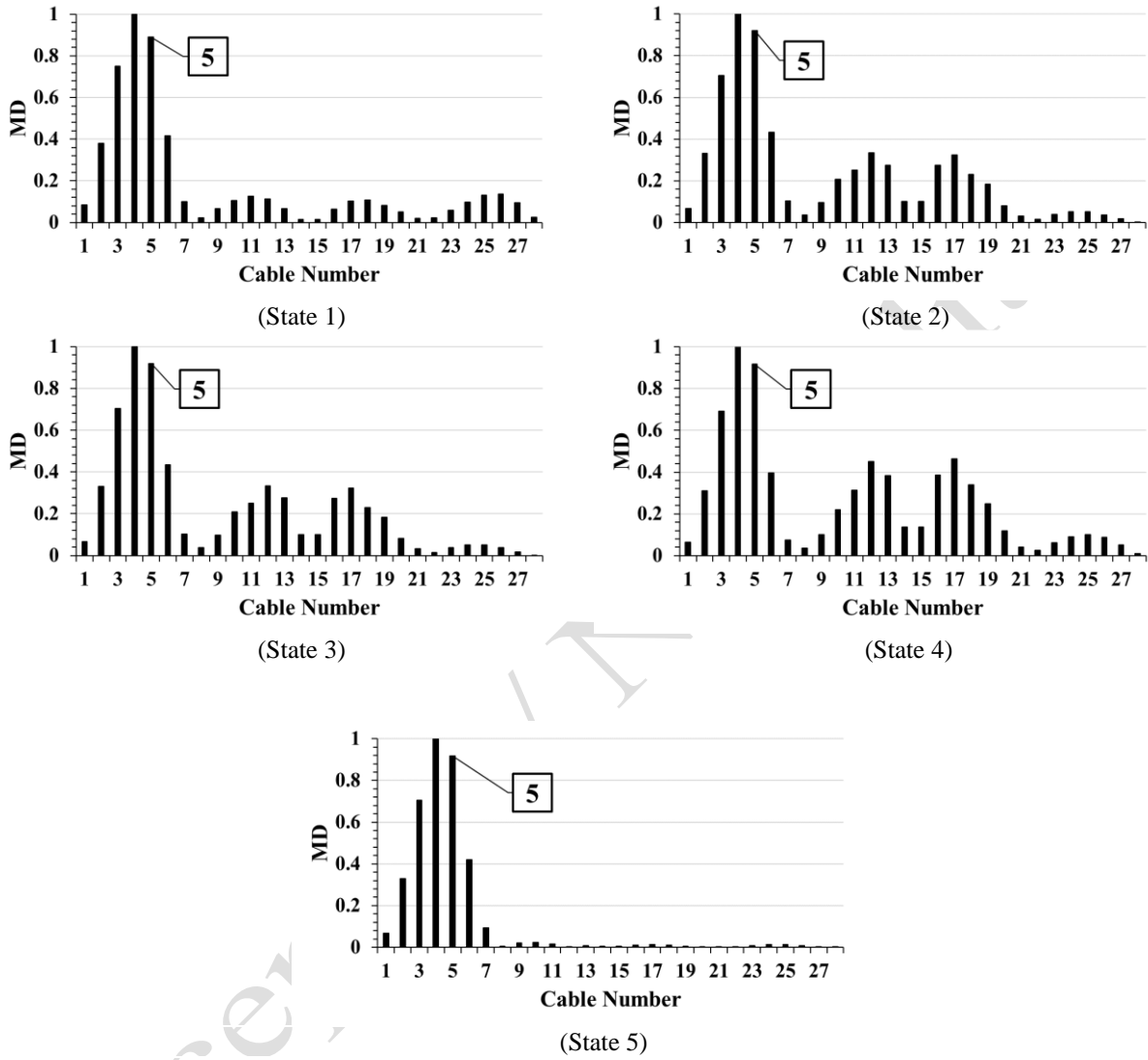
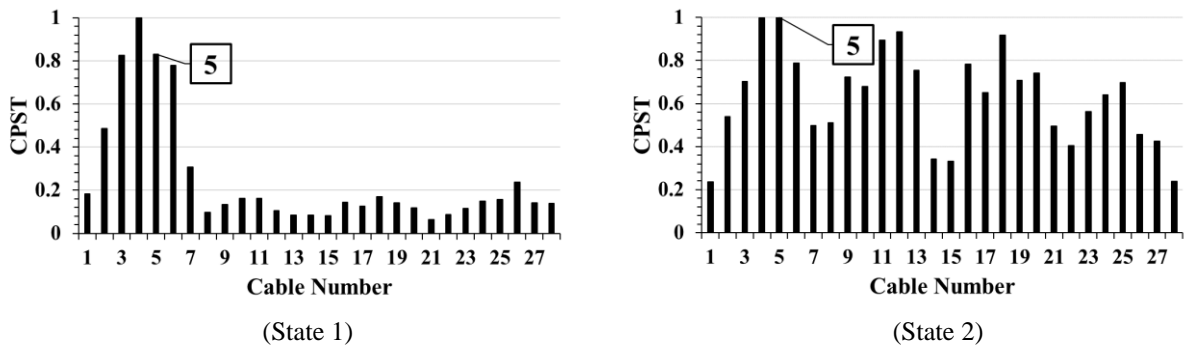


Fig.9. Mahalanobis Distance (MD) curves of cable 5 for five states



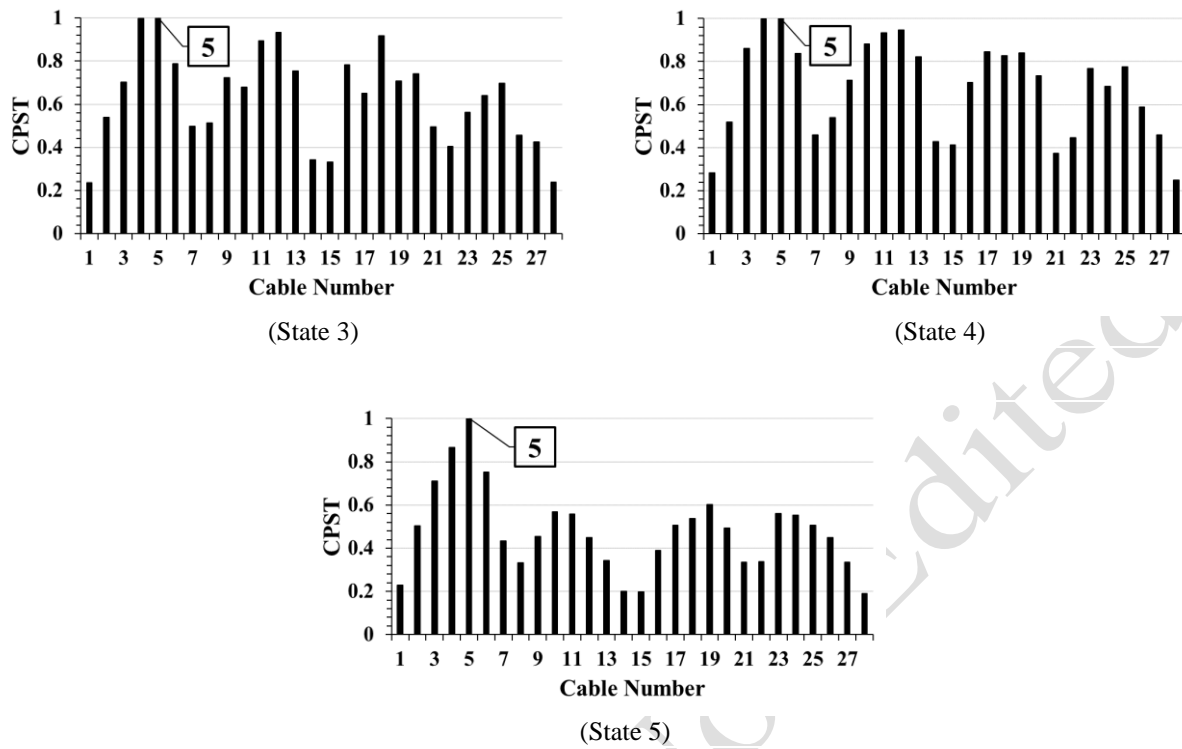
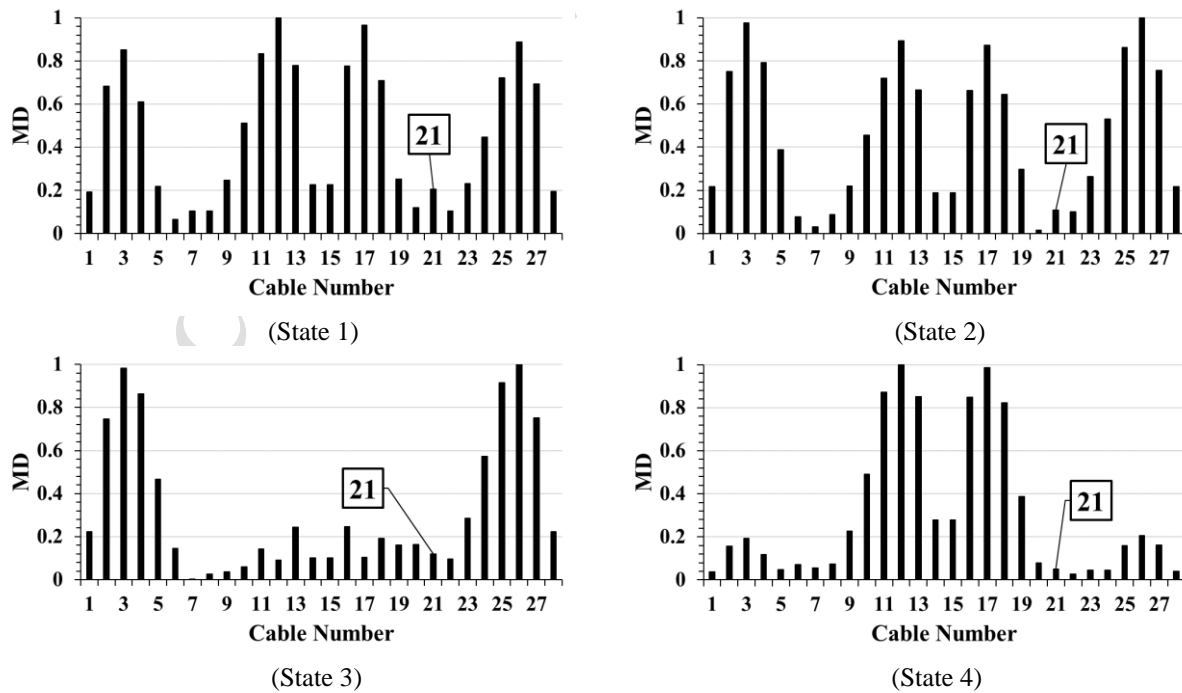


Fig. 10. Change in Phase Space Topology (CPST) curves of cable 5 for five states



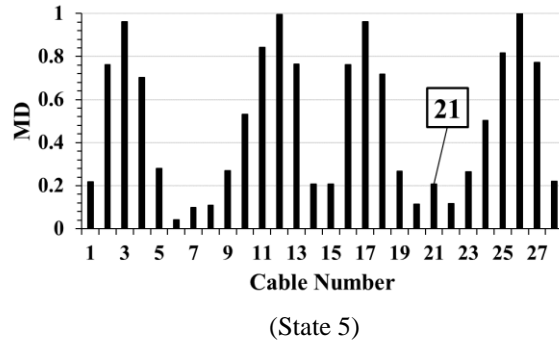


Fig. 11. Mahalanobis Distance (MD) curves of cable 21 for five states

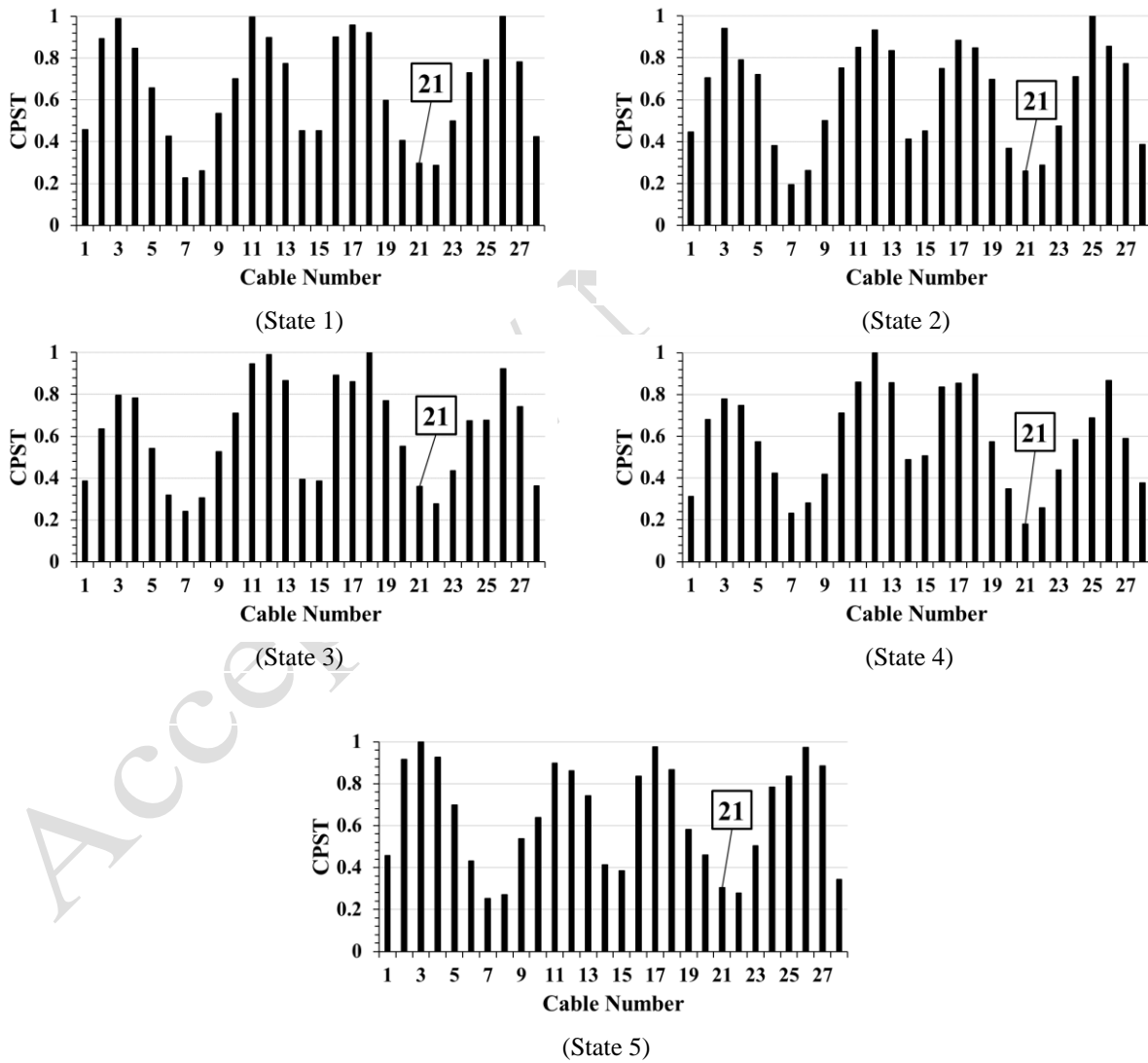


Fig. 12. Change in Phase Space Topology (CPST) curves of cable 21 for five states

The summary of results evaluation for MD and CPST damage indexes is presented in Table 7. Out of 100 analyses conducted, MD correctly identified 24% of scenarios when the cable damage level was 20%, while CPST correctly identified 12% of scenarios. For a damage level of 30%, these values increased to 31% for MD and 28% for CPST. When the damage level was 40%, MD and CPST indexes demonstrated the ability to detect 34% and 35% of the damaged cables across various states, respectively. Moreover, a significant percentage of the diagnoses were near the damaged cable. The MD index showed an accuracy of approximately 56%, considering both accurately and nearly detected cases for the 40% damage level.

**Table 7.** Summary of MD and CPST evaluation

Damage percentage	20%		30%		40%	
Damage index	MD	CPST	MD	CPST	MD	CPST
Total number of analyses	100	100	100	100	100	100
Exactly detected	24	12	31	28	34	35
Nearly detected	15	14	19	20	22	12
Accuracy	39%	26%	50%	48%	56%	47%

#### 4.1. Comparison with Modal-Based Methods

To highlight the robustness of the phase space-based damage detection method, a comparative analysis between CPST and modal parameters was conducted. CPST was derived from the displacement measurements at three distinct points on the deck, as shown in Figure 13: near the support in the first span (point 1), adjacent to the pylon (point 2), and in proximity to the support in the second span (point 3). It was meticulously examined across damage levels of 10% to 50% for cable number 25 under all five aforementioned states. Modal parameters such as the frequency of the bridge's first mode and Modal Assurance Criterion (MAC) were analyzed. All indexes were normalized as follows (Nie et al., 2013):

$$CPST_{norm} = \frac{|CPST^d - CPST^u|}{CPST^u} \quad (10-1)$$

$$\omega_{norm} = \frac{|\omega^d - \omega^u|}{\omega^u} \quad (10-2)$$

$$MAC_{norm} = \frac{|MAC^d - MAC^u|}{MAC^u}, \quad MAC = \frac{\{(\varphi^u)^T \varphi^d\}^2}{\{(\varphi^u)^T \varphi^u\} \{(\varphi^d)^T \varphi^d\}} \quad (10-3)$$

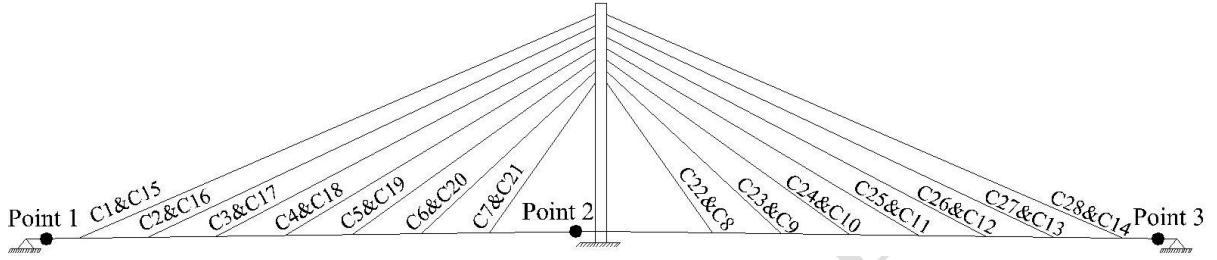
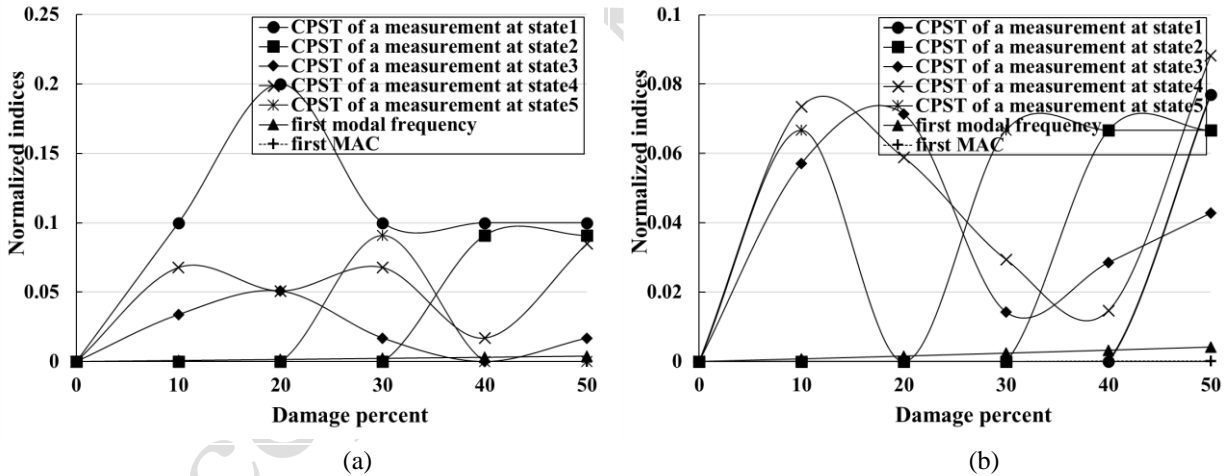
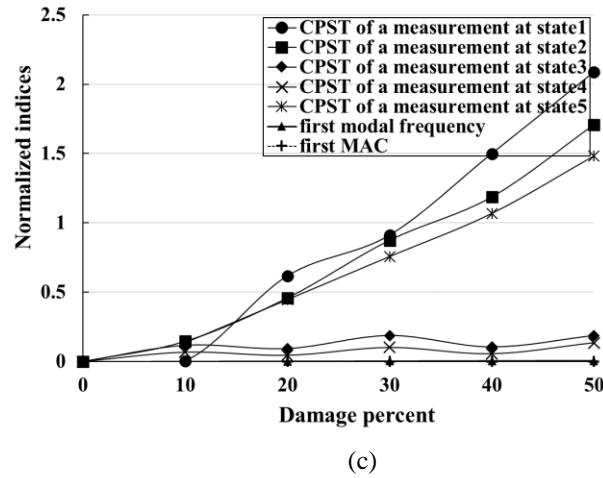


Fig. 13. Location of measurement points





**Fig. 14.** A comparison of the normalized CPST and modal parameters: (a) measurement point 1; (b) measurement point 2 and (c) measurement point 3

The subscripts ‘u’ and ‘d’ denote the healthy and damaged cases, respectively.  $\varphi$  refers to the mode shape. Figures 14(a) and 14(b) illustrate the CPST index values and the modal parameters at point 1 in the first span and point 2 adjacent to the pylon. CPST exhibited heightened sensitivity to damage compared to frequency analysis. While CPST may not consistently specify the exact location of damaged cables under different load patterns and speeds, its changes were much more noticeable than those of the first mode frequency and MAC coefficient. Although they have served as significant indicators of structural damage. Figure 14(c) depicts the results from point 3, which is situated near the damaged cable. Based on the previous analysis, a noticeable correlation was observed between the CPST values and increasing damage levels across load-passing states 1, 2, and 5. For instance, at the 10% damage level, the accuracy of CPST increased by 84.5% compared to the first mode frequency of the structure across load state 1. CPST emerged as a powerful index for identifying damage in cable-stayed bridges, showcasing its robustness regardless of the location of the damage.

---

## 5. Conclusion and Future Work

A method for assessing cable health in cable-stayed bridges using phase space analysis was introduced. The proposed approach was validated through comprehensive numerical investigations conducted on the Manavgat cable-stayed bridge. The evaluation encompassed a range of scenarios, which included various loading patterns and speeds. The combination of two indexes, namely the Change in Phase Space Topology (CPST) and Mahalanobis Distance (MD), was used for damage detection by identifying subtle deviations in phase space trajectories. Some important conclusions are summarized as follows:

- The damage indexes accurately identified the most damaged cables in scenarios where the passing load was the same in both healthy and damaged cases. However, cables near the pylon and backstay cables presented challenges due to their interconnected role.
- The MD Index displayed accuracy ranging from 39% to 56% for damage levels of 20% to 40% under various loading patterns and speeds, while the CPST Index achieved accuracy between 26% and 47%. In many cases, these indexes detected cables adjacent to the damaged cable, effectively identifying the location of the damage. In states where the T5A truck passed at higher speeds, the indexes demonstrated superior effectiveness.
- Some scenarios involving cables near the pylon challenged the MD and CPST in detecting damage, resulting in inconclusive responses. For damage levels of 30% and above, improved results were noted, indicating the method's heightened sensitivity to higher levels of damage.
- The comparison with modal parameters highlighted the enhanced sensitivity of CPST, derived from the phase-space response method, in detecting damage within the time

---

domain. CPST was presented as a valuable tool for monitoring the health of cable-stayed bridges, even when the measurement point is distant from the damage location.

This paper presented an initial approach for a practical solution aimed at ensuring the health of cable-stayed bridges and exploring real-world implementations. Suggestions for enhancing this method in the future include incorporating dynamic effects from high-speed loading, refining parameters with increased precision and sensitivity (especially concerning backstay cables and those near the pylon), and considering different load placement locations within the passing lanes.

## Declaration of Competing Interest

The authors declare that they have no known competing financial interests or personal relationships that could have appeared to influence the work reported in this paper.

## 6. References

- AASHTO. (2008). *LRFD Bridge Design Specifications*, Washington, DC.
- Abarbanel, H. (2012). *Analysis of Observed Chaotic Data*, Springer Science & Business Media.
- Australasian Railway Association. (1992). *Bridge Design Code*, Austroads, Sydney, Australia.
- Bakhshizadeh, A. and Sadeghi, K. (2023). “Health-monitoring methods for long-span cable-stayed bridges”, *Infrastructure Asset Management*, 11(1), 41–54, <https://doi.org/10.1680/jinam.23.00030>.
- Bakhshizadeh, A., Sadeghi, K., Ahmadi, S. and Royaei, J. (2023). “Damage Identification in Long-Span Cable-Stayed Bridges Under Multiple Support Excitations”, *International Journal of Civil Engineering*, 21, 1275–1290, <https://doi.org/10.1007/s40999-023-00823-7>.
- Bedon, C., Dilena, M. and Morassi, A. (2016). “Ambient vibration testing and structural identification of a cable-stayed bridge”, *Meccanica*, 51(11), 2777–2796, <https://doi.org/10.1007/s11012-016-0430-2>.
- Broomhead, D.S. and King, G.P. (1986). “Extracting qualitative dynamics from experimental data”, *Physica D: Nonlinear Phenomena*, 20(2–3), 217–236, [https://doi.org/10.1016/0167-2789\(86\)90031-X](https://doi.org/10.1016/0167-2789(86)90031-X).

- 
- Cheng, Y., Su, Z. and Zhang, J. (2024). “Mode shape-aided cable force estimation of a double-hanger system using a vision-based monitoring method”, *Measurement*, 227, 114214, <https://doi.org/10.1016/j.measurement.2024.114214>.
- Elkady, A.Z., Youssef, A.F., Abuelnadr, I., DePeder, D. and Seleemah, A.A. (2023). “Optimum Location of Seismic Isolation for Manavgat Cable-Stayed Bridge”, *International Journal of Advanced Engineering, Management and Science*, 9(11), 39–58, <https://dx.doi.org/10.22161/ijaems.911.3>.
- Fathali, M.A., Dehghani, E. and Hoseini Vaez, S.R. (2020). “An approach for adjusting the tensile force coefficient in equivalent static cable-loss analysis of the cable-stayed bridges”, *Structures*, 25, 720–729, <https://doi.org/10.1016/j.istruc.2020.03.054>.
- George, R.C., Mishra, S.K. and Dwivedi, M. (2018). “Mahalanobis distance among the phase portraits as damage feature”, *Structural Health Monitoring*, 17(4), 869–887, <https://doi.org/10.1177/1475921717722743>.
- He, W.-Y., Ren, W.-X. and Zhu, S. (2017). “Baseline-free damage localization method for statically determinate beam structures using dual-type response induced by quasi-static moving load”, *Journal of Sound and Vibration*, 400, 58–70, <https://doi.org/10.1016/j.jsv.2017.03.049>.
- He, Z., Li, W., Salehi, H., Zhang, H., Zhou, H. and Jiao, P. (2022). “Integrated structural health monitoring in bridge engineering”, *Automation in Construction*, 136, 104168, <https://doi.org/10.1016/j.autcon.2022.104168>.
- Hong, W., Wu, Z., Yang, C., Wan, C. and Wu, G. (2012). “Investigation on the damage identification of bridges using distributed long-gauge dynamic macrostrain response under ambient excitation”, *Journal of Intelligent Material Systems and Structures*, 23(1), 85–103, <https://doi.org/10.1177/1045389X11430743>.
- Jana, D., Nagarajaiah, S. and Yang, Y. (2022). “Computer vision-based real-time cable tension estimation algorithm using complexity pursuit from video and its application in Fred-Hartman cable-stayed bridge”, *Structural Control and Health Monitoring*, 29(9), e2985, <https://doi.org/10.1002/stc.2985>.
- Jiang, A.-H., Huang, X.-C., Zhang, Z.-H., Li, J., Zhang, Z.-Y. and Hua, H.-X. (2010). “Mutual information algorithms”, *Mechanical Systems and Signal Processing*, 24(8), 2947–2960, <https://doi.org/10.1016/j.ymssp.2010.05.015>.
- Kordi, A. and Mahmoudi, M. (2022). “Damage detection in truss bridges under moving load using time history response and members influence line curves”, *Civil Engineering Infrastructures Journal*, 55(1), 183–194, <https://doi.org/10.22059/cej.2021.314109.1723>.
- Lei, X., Siringoringo, D.M., Sun, Z. and Fujino, Y. (2023). “Displacement response estimation of a cable-stayed bridge subjected to various loading conditions with one-dimensional residual convolutional autoencoder method”, *Structural Health Monitoring*, 22(3), 1790–1806, <https://doi.org/10.1177/14759217221116637>.
- Li, D., Cao, M., Manoach, E., Jia, H., Ragulskis, M., Shen, L. and Sha, G. (2021). “A multiscale reconstructed attractors-based method for identification of structural damage under impact excitations”, *Journal of Sound and Vibration*, 495, 115925, <https://doi.org/10.1016/j.jsv.2020.115925>.

- 
- Li, S., Li, H., Liu, Y., Lan, C., Zhou, W. and Ou, J. (2014). “SMC structural health monitoring benchmark problem using monitored data from an actual cable-stayed bridge”, *Structural Control and Health Monitoring*, 21(2), 156–172, <https://doi.org/10.1002/stc.1559>.
- De Maesschalck, R., Jouan-Rimbaud, D. and Massart, D.L. (2000). “The mahalanobis distance”, *Chemometrics and Intelligent Laboratory Systems*, 50(1), 1–18, [https://doi.org/10.1016/S0169-7439\(99\)00047-7](https://doi.org/10.1016/S0169-7439(99)00047-7).
- Nazarian, E., Ansari, F. and Azari, H. (2016). “Recursive optimization method for monitoring of tension loss in cables of cable-stayed bridges”, *Journal of Intelligent Material Systems and Structures*, 27(15), 2091–2101, <https://doi.org/10.1177/1045389X15620043>.
- Nichols, J.M. (2003). “Structural health monitoring of offshore structures using ambient excitation”, *Applied Ocean Research*, 25(3), 101–114, <https://doi.org/10.1016/j.apor.2003.08.003>.
- Nie, Z., Hao, H. and Ma, H. (2012). “Using vibration phase space topology changes for structural damage detection”, *Structural Health Monitoring*, 11(5), 538–557, <https://doi.org/10.1177/1475921712447590>.
- Nie, Z., Hao, H. and Ma, H. (2013). “Structural damage detection based on the reconstructed phase space for reinforced concrete slab: Experimental study”, *Journal of Sound and Vibration*, 332(4), 1061–1078, <https://doi.org/10.1016/j.jsv.2012.08.024>.
- Pamwani, L. and Shelke, A. (2018). “Damage Detection Using Dissimilarity in Phase Space Topology of Dynamic Response of Structure Subjected to Shock Wave Loading”, *Journal of Nondestructive Evaluation, Diagnostics and Prognostics of Engineering Systems*, 1(4), 1–13, <https://doi.org/10.1115/1.4040472>.
- Pan, H., Azimi, M., Yan, F. and Lin, Z. (2018). “Time-Frequency-Based Data-Driven Structural Diagnosis and Damage Detection for Cable-Stayed Bridges”, *Journal of Bridge Engineering*, 23(6), [https://doi.org/10.1061/\(ASCE\)BE.1943-5592.0001199](https://doi.org/10.1061/(ASCE)BE.1943-5592.0001199).
- Paul, B., George, R.C. and Mishra, S.K. (2017). “Phase space interrogation of the empirical response modes for seismically excited structures”, *Mechanical Systems and Signal Processing*, 91, 250–265, <https://doi.org/10.1016/j.ymssp.2016.12.008>.
- Peng, Z., Li, J. and Hao, H. (2022). “Data driven structural damage assessment using phase space embedding and Koopman operator under stochastic excitations”, *Engineering Structures*, 255, 113906, <https://doi.org/10.1016/j.engstruct.2022.113906>.
- Prawin, J., Lakshmi, K. and Rao, A.R.M. (2020). “Structural damage diagnosis under varying environmental conditions with very limited measurements”, *Journal of Intelligent Material Systems and Structures*, 31(5), 665–686, <https://doi.org/10.1177/1045389X19898268>.
- Rhodes, C. and Morari, M. (1997). “The false nearest neighbors algorithm: An overview”, *Computers & Chemical Engineering*, 21, S1149–S1154, [https://doi.org/10.1016/S0098-1354\(97\)87657-0](https://doi.org/10.1016/S0098-1354(97)87657-0).
- Rinaldi, C., Lepidi, M., Potenza, F. and Gattulli, V. (2023). “Identification of cable tension through physical models and non-contact measurements”, *Mechanical Systems and Signal Processing*, 205, 110867, <https://doi.org/10.1016/j.ymssp.2023.110867>.

- Saidin, S.S., Kudus, S.A., Jamadin, A., Anuar, M.A., Amin, N.M., Ya, A.B.Z. and Sugiura, K. (2023). “Vibration-based approach for structural health monitoring of ultra-high-performance concrete bridge”, *Case Studies in Construction Materials*, 18, e01752, <https://doi.org/10.1016/j.cscm.2022.e01752>.
- Takens, F. (1981). “Detecting strange attractors in turbulence”, *Dynamical Systems and Turbulence*, Warwick, Berlin, Heidelberg, <https://doi.org/10.1007/BFb0091924>.
- Tuttipongawat, P., Sasaki, E., Suzuki, K., Fukuda, M., Kawada, N. and Hamaoka, K. (2019). “PC tendon damage detection based on phase space topology changes in different frequency ranges”, *Journal of Advanced Concrete Technology*, 17(8), 474–488, <https://doi.org/10.3151/jact.17.474>.
- Wu, B., Wu, G., Lu, H. and Feng, D. (2017). “Stiffness monitoring and damage assessment of bridges under moving vehicular loads using spatially-distributed optical fiber sensors”, *Smart Materials and Structures*, 26(3), 35058, <https://doi.org/10.1088/1361-665X/aa5c6f>.
- Wu, B., Wu, G. and Yang, C. (2019). “Parametric study of a rapid bridge assessment method using distributed macro-strain influence envelope line”, *Mechanical Systems and Signal Processing*, 120, 642–663, <https://doi.org/10.1016/j.ymsp.2018.10.039>.
- Yu, C.P. (2020). “Tension prediction for straight cables based on effective vibration length with a two-frequency approach”, *Engineering Structures*, 222, 111121, <https://doi.org/10.1016/j.engstruct.2020.111121>.
- Zarraf, S.E.H.A.M., Norouzi, M., Allemang, R.J., Hunt, V.J., Helmicki, A. and Venkatesh, C. (2018). “Ironton-Russell Bridge: Application of Vibration-Based Cable Tension Estimation”, *Journal of Structural Engineering*, 144(6), 04018066, [https://doi.org/10.1061/\(asce\)st.1943-541x.0002054](https://doi.org/10.1061/(asce)st.1943-541x.0002054).
- Zhang, H., Mao, J., Wang, H., Zhu, X., Zhang, Y., Gao, H., Ni, Y., *et al.* (2023). “A novel acceleration-based approach for monitoring the long-term displacement of bridge cables”, *International Journal of Structural Stability and Dynamics*, 23(05), 2350053, <https://doi.org/10.1142/S0219455423500530>.
- Zhang, L., Wu, G. and Cheng, X. (2020). “A rapid output-only damage detection method for highway bridges under a moving vehicle using long-gauge strain sensing and the fractal dimension”, *Measurement: Journal of the International Measurement Confederation*, 158, 107711, <https://doi.org/10.1016/j.measurement.2020.107711>.
- , W., Li, J., Hao, H. and Ma, H. (2017). “Damage detection in bridge structures under moving loads with phase trajectory change of multi-type vibration measurements”, *Mechanical Systems and Signal Processing*, 87(A), 410–425, <https://doi.org/10.1016/j.ymsp.2016.10.035>.

## Nomenclature

- T = The time lag of phase space reconstruction
- d = Embedding dimension of phase space reconstruction

---

$N$	=	Data points of a time series
$X(n)$	=	Reconstructed phase space for the healthy case
$Y(n)$	=	Reconstructed phase space for the damaged case
$Y(r)$	=	A fiducial point in the damaged case
$p$	=	Total neighborhood numbers of the fiducial point
$NN$	=	The nearest neighbor points to the fiducial point
$\square$ $Y(r)$	=	The fiducial point in the predicted damaged case
$nt$	=	Number of repeats or fiducial points to obtain a reasonable estimation of CPST
$[X]$	=	Matrix of the healthy case
$[Y]$	=	Matrix of the damaged case
$\{X\}$	=	Healthy phase portrait vector
$\{Y\}$	=	Damaged phase portrait vector
$\{\mu\}_X$	=	Mean vector of the healthy phase portrait
$\{\mu\}_Y$	=	Mean vector of the damaged phase portrait
$[C_{XX}]$	=	The covariance matrix of the healthy phase portrait
$[C_{YY}]$	=	The covariance matrix of the damaged phase portrait
$[C_{ww}]$	=	Weighted covariance matrix
$W$	=	Weight factor
$L$	=	Distance between point loads
$V$	=	Speed of the passing load
$\Delta t$	=	Time taken to traverse $L$ distance at speed $V$
$\omega$	=	Modal frequency
$\varphi$	=	Mode shape

---

*Accepted / Not Edited*